

SUPPLEMENTARY MATERIALS

Anonymous authors

Paper under double-blind review

1 COMPARISON WITH STATE-OF-THE-ART METHODS

Table 1: Performance of Fast-SNN, Offset, and CSS on ImageNet after converting 3-bit VGG-16

Methods	T=1	T=2	T=3	T=4
Offset (rate)	64.90% (129 steps)	70.85% (130 steps)	72.06% (131 steps)	72.53% (132 steps)
Fast-SNN (rate)	3.19% (1 steps)	52.74% (2 steps)	68.13% (3 steps)	71.26% (4 steps)
CSS	2.87% (17 steps)	68.53% (18 steps)	72.81% (19 steps)	73.25% (20 steps)
Methods	T=5	T=6	T=7	T=8
Offset (rate)	72.79% (133 steps)	72.92% (134 steps)	73.05% (1235 steps)	73.01% (136 steps)
Fast-SNN (rate)	72.21% (5 steps)	72.64% (6 steps)	72.87% (7 steps)	72.97% (8 steps)
CSS	73.23% (21 steps)	73.24% (22 steps)	73.23% (23 steps)	73.24% (24 steps)

Table 2: Performance of Fast-SNN, Offset, and CSS on ImageNet after converting 2-bit VGG-16

Methods	T=1	T=2	T=3	T=4
Offset (rate)	68.44% (65 steps)	71.71% (66 steps)	72.39% (67 steps)	72.54% (68 steps)
Fast-SNN (rate)	23.82% (1 steps)	66.98% (2 steps)	70.99% (3 steps)	71.92% (4 steps)
CSS	19.49% (17 steps)	71.22% (18 steps)	72.31% (19 steps)	72.56% (20 steps)

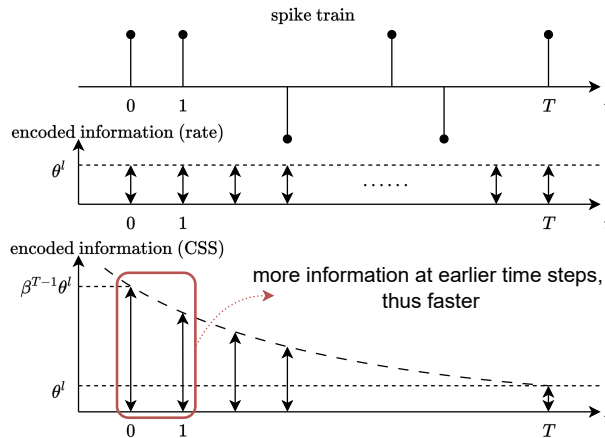


Figure 1: CSS coding assigns more weight to earlier spikes, allowing it to achieve higher performance than rate coding while using fewer time steps.

2 THE ROLE OF NEGATIVE SPIKES

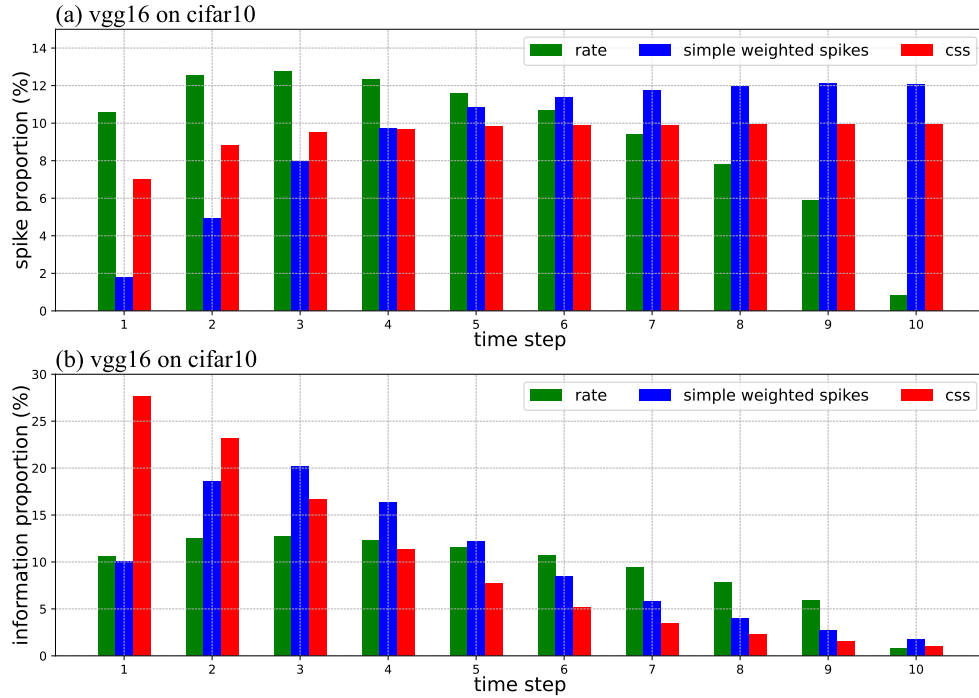


Figure 2: (a) The distribution of spikes across different time steps. Green represents rate coding. Blue represents the case after spike weighting, where the spikes are concentrated in the later time steps. Red represents the case in CSS coding, where we successfully shifted the distribution of weighted spikes toward earlier time steps. (b) The distribution of fired information across different time steps.

Table 3: Changes in accuracy before and after introducing negative spikes. Experiments were performed using VGG-16 on CIFAR-10.

Coding Scheme	Negative Spikes	T=2	T=4	T=6	T=8
rate	×	10.00%	47.48%	94.25%	95.26%
CSS	×	90.93%	92.94%	93.12%	93.22%
rate	✓	10.21%	47.88%	94.42%	95.34%
CSS	✓	95.14%	95.55%	95.60%	95.58%

3 ENERGY CONSUMPTION ANALYSIS

Table 4: Energy consumption of VGG-structured SNNs on CIFAR-10

Methods	Arch.	Accuracy	T	Latency	SyOP (ACs)	MACs	Energy Consumption
ANN	VGG-11	93.82%	N/A	N/A	0	153.2M	0.7047mJ
CSS	VGG-11	93.78%	8	19	0	132.4M	0.1191mJ
ANN	VGG-16	95.88%	N/A	N/A	0	313.88M	1.4438mJ
TTFS	VGG-16	93.53%	64	1024	120.53M	0	0.1085mJ
CSS	VGG-16	95.84%	8	24	308.35M	0	0.2775mJ
CSS	VGG-16	95.14%	2	18	102.19M	0	0.0920mJ

Table 5: Energy consumption of Fast-SNN and CSS on CIFAR10 after converting 3-bit ResNet-18.

Methods	Accuracy	T	Latency	SyOP (ACs)	MACs	Energy Consumption
ANN	95.25%	N/A	N/A	0	2.22G	10.21mJ
Fast-SNN (rate)	95.42%	7	7	1.02G	12.42M	0.9751mJ
Fast-SNN (rate)	95.23%	6	6	878.3M	10.65M	0.8395mJ
CSS	95.31%	3	21	730.65M	1.84M	0.6660mJ
CSS	95.24%	2	20	489.93M	1.91M	0.4497mJ

4 SELECTION OF THE AMPLIFICATION COEFFICIENT

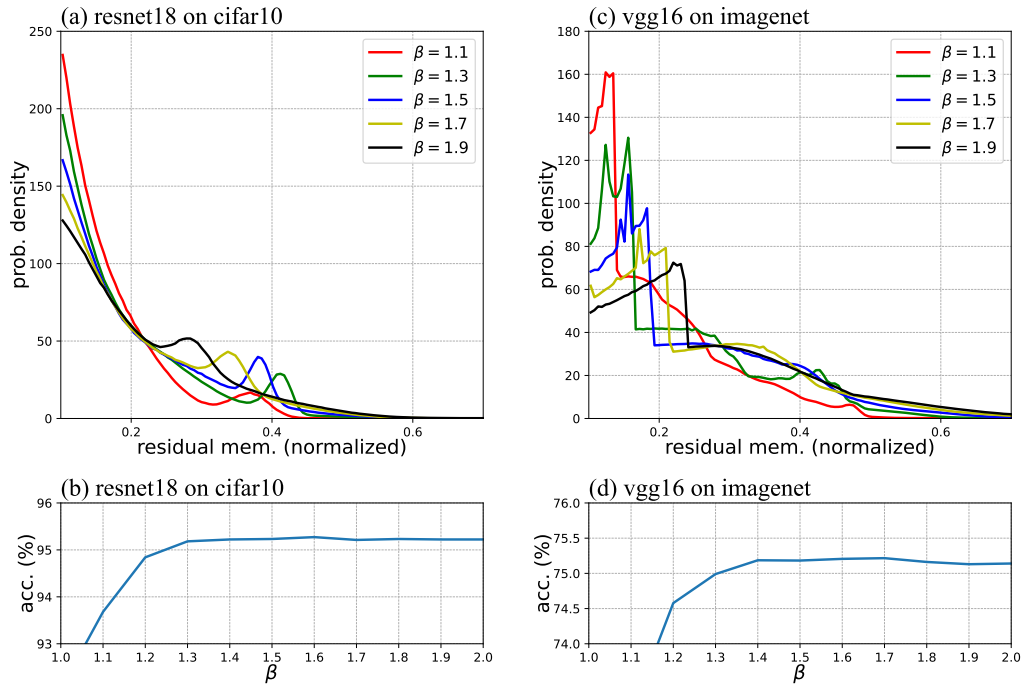


Figure 3: Impact of amplification coefficient on residual membrane potential and accuracy. All the membrane potentials are normalized. Note the firing threshold is 0.5. For ResNet-18 on CIFAR-10: (a) Residual membrane potential distributions under different β . (b) Accuracy variations corresponding to different β . For VGG-16 on ImageNet: (c) Residual membrane potential distributions under different β . (d) Accuracy variations corresponding to different β .